Jurnal Tribologi 30 (2021) 100-115

Analysis of electrorheological fluid operated symmetric journal bearing

Sunil Kumar *, Vijay Kumar, Anoop K. Singh

Chitkara University Institute of Engineering and Technology, Chitkara University, Punjab 140401, INDIA.
*Corresponding author: sunil.sharma@chitkara.edu.in

KEYWORDS

Electrorheological fluid
Journal bearing
Finite element method
Performance characteristics

ABSTRACT

Hole entry journal bearing with symmetric configuration has been analyzed in the present work using finite element method. Electrorheological fluid (ERF) was used as a lubricant and orifice restrictors were selected as flow control devices. Performance characteristics such as fluid film pressure, fluid film thickness and bearing flow were investigated for ERF operated journal bearing and results were compared with Newtonian case. Using ERF, very precise control over the lubricant viscosity has been observed by altering electric field. Pressure distribution curves were plotted over the entire bearing circumference. Higher pressure values were obtained for ERF operated bearing compared to Newtonian lubricated bearing. It has been found that the pressure increased with increase in voltage for ERF. Decrease in bearing flow has been observed by increasing electric field.

NOMENCLATURE

α, β	circumferential and longitudinal coordinates	$\bar{p}_{max}$	maximum fluid film pressure
$\overline{X_J}, \overline{Z_J}$	journal center position	$\bar{h}_{min}$	minimum film thickness
$\bar{p}$	fluid pressure	$\bar{\mu}_0$	zero field viscosity
Ω	journal rotational speed	$\bar{\mu}_r$	reference viscosity
$\bar{C}_{s2}$	restrictor design parameter	$\bar{\tau}_0$	yield stress
$\bar{p}_c$	pressure at holes	$\bar{\dot{\gamma}}$	shear rate
$\bar{F}_0, \bar{F}_1, \bar{F}_2$	viscosity functions	c	radial clearance
$\bar{\mu}$	lubricant dynamic viscosity	R_J	journal radius

Received 14 July 2021; received in revised form 3 August 2021; accepted 29 August 2021.
To cite this article: Kumar et al. (2021). Analysis of electrorheological fluid operated symmetric journal bearing. Jurnal Tribologi 30, pp.100-115.

$\{\bar{R}_x\}, \{\bar{R}_z\}$	vectors due to journal center velocity	p_s	supply pressure
$\bar{Q}_R$	flow through restrictor	PERR	percentage error
$[\bar{F}]$	fluidity matrix	ε	eccentricity ratio
$\{\bar{P}\}$	pressure vector	F	resultant force
$\{\bar{Q}\}$	flow vector	E	electric field strength
$\{\bar{R}_H\}$	vector for hydrodynamic terms	V	applied voltage
$\bar{W}$	radial load	A	ERF parameter
$\bar{h}$	fluid film thickness	B	ERF constant

1.0 INTRODUCTION

The performance of journal bearings depends upon the behavior of lubricants used in bearing system. Kumar et al., (2020a) presented the detailed study of lubricants and their impact on the journal bearing performance. The Electrorheological fluid (ERF) has been considered as an effective lubricant for performance enhancement of journal bearings Dimarogonas et al., (1992). Electrorheological fluid is a smart fluid in which the dynamic viscosity of the fluid changes as a result of imposition of electrical field. The rheological behavior of ERF depends upon the electrical field strength. More the electric field strength, more will be ER effect. It has been observed that the ERF may convert the ordinary journal bearing to a smart journal bearing. A smart journal bearing means a bearing system which is capable to alter the performance characteristics as per requirement without changing the bearing design. ERF is highly suitable to fulfil such bearing system requirements. Due to the quick response of ERF, very precise control over the journal bearing can be made. Other than journal bearing applications, ERF is applicable for the automotive parts such as shock absorbers, engine mounts and clutches.

Researchers were involved in high-speed journal bearing analysis using computational fluid dynamics (CFD) (Rasep et al. 2021; Muchammad, 2021) finite element methods (FEM) (Garg, 2015; Yadav, 2018) and Artificial Neural network (ANN) (Kumar et al., 2020b). ERF has been used as a smart lubricant for journal bearing in the recent past (Nikolakopoulos and Papadopoulos 1998; Peng and Zhu, 2005; Jang and Tichy 1997). Kollias and Dimarogonas, (1994) studied the influence of ERF on low-speed journal bearing and studied the fluid film pressure distribution.

They found that the ERF has similar behavior as Bingham fluid model. Nikolakopoulos and Papadopoulos, (1996) experimentally investigated the effect of ERF on the performance of journal bearing. They showed that the ERF at high shear rate follow the Bingham model in bearings. Basavaraja et al., (2010) conducted a theoretical study to check the journal misalignment on the static and dynamic performance of ERF operated journal bearing. They concluded that the reduction in bearing characteristics parameters was partially compensated by using ERF as a lubricant. Giant Electrorheological Fluid (GERF) has been proposed by researchers as a best smart fluid for journal bearings due to its excellent lubricant characteristics (Nikolakopoulos and Papadopoulos, 1996; Basavaraja et al., 2010).

Analysis of hole entry journal bearing with micropolar lubricant (Ram, 2016) and couple stress lubricant (Ram, 2017) has been performed in recent past. Kumar and Sharma, (2019) analyzed the load capacity, lubricant film thickness and stiffness coefficients for conical journal bearing and found that values of these attributes increased using ERF as a bearing lubricant. Tomar and Sharma, (2020) performed the finite element analysis for grooved surface journal bearings using ERF as a bearing lubricant and concluded that the ERF increased the minimum lubricant film thickness and stiffness coefficient values. Agarwal and Sharma, (2021) analyzed spherical thrust

bearing using FEM to determine the impact of axial eccentricity and ERF together on the bearing performance. The increase in performance has been obtained for negative axial eccentricity. Present investigation and literature study have proved that ERF can be used as an effective lubricant to enhance the static and dynamic characteristics of various configurations of journal bearing systems.

In previous work, the electrorheological fluids were analyzed for various bearing configurations but not for the configuration selected in present work. The design data has not been available for orifice compensated symmetric hole entry configuration of hybrid journal bearing in the available literature. The static performance characteristics of hole entry bearing operated with ERF is analyzed and presented in this paper. Finite Element analysis is performed to solve the flow governing Reynold's equation. The performance characteristics such as maximum fluid film pressure ($\bar{p}_{max}$), minimum fluid film thickness ($\bar{h}_{min}$), bearing flow ($\bar{Q}$) and eccentricity ratio (ε) are analyzed numerically. The external applied radial load ($\bar{W}$), journal rotational speed (Ω) and dynamic viscosity (μ) of the ERF are considered as the input parameters in present study.

2.0 ELECTRORHEOLOGICAL FLUID MODEL

An Electrorheological fluid (ERF) consists of very small sized (<50 μm) electrically conductive particles in non-conducting oil. When electric field is introduced, the particles change their rheological behavior rapidly. Due to electrorheological (ER) effect, the randomly dispersed electric conductive particles become polarized. They form a chain when interacting with each other (Conrad and Sprecher, 1991; Hao, 2001; Hao, 2002).

The fluid state changes to semi solid due to the increase in yield stress which is the result of electric field strength. More the yield stress, more will be the apparent fluid viscosity. This increases the yield strength of the fluid. The behavior of ERF is shown in Figure 1. The behavior of ERF is governed by Bingham model. This model was proposed by (Dorier and Tichy, 1992). Bearing parameters and lubricant properties used in present analysis are tabulated in Table 1. In presence of electric field, particles arranged themselves in a chain-like structure. The fluid state changes to semi solid. The dimensional Bingham model equation can be written as eq. 1;

$$\mu(\dot{\gamma}) = \mu_0 + \frac{2\tau_0}{\pi\dot{\gamma}} \tan^{-1}\left(\frac{\dot{\gamma}}{\dot{\gamma}_0}\right) \quad (1)$$

where τ_0 is yield stress which can be written as eq. 2;

$$\tau_0(E) = A\, E^B \quad (2)$$

The electric field is determined by the following relation given in eq. 3;

$$E = \frac{V}{h} \quad (3)$$

where V is applied voltage and h is thickness of lubricant layer.
Parameters used to express the model in non-dimensional form are given in eq. 4;

$$\bar{\mu}_0 = \frac{\mu_0}{\mu_r}; \bar{\tau}_0 = \tau_0\left(\frac{R_J}{c\, p_s}\right); \bar{\dot{\gamma}} = \dot{\gamma}\left(\frac{c\, p_s}{\mu_r R_J}\right) \quad (4)$$

Hence, non-dimensional model equation can be written as eq. 5;

$$\bar{\mu}_a = \bar{\mu}(\bar{\dot{\gamma}}) = \bar{\mu}_0 + \frac{2\bar{\tau}_0}{\pi\bar{\dot{\gamma}}}\tan^{-1}\left(\frac{\bar{\dot{\gamma}}}{\bar{\dot{\gamma}}_0}\right) \quad (5)$$

where $\bar{\mu}_a$ is the apparent fluid viscosity.
Non-dimensional shear rate ($\bar{\dot{\gamma}}$) can be written as eq. 6;

$$\bar{\dot{\gamma}} = \left[\left(\frac{\bar{h}}{\bar{\mu}}\frac{\partial\bar{p}}{\partial\alpha}\left(\bar{z} - \frac{\bar{F}_1}{\bar{F}_0}\right) + \frac{\Omega}{\bar{\mu}\,\bar{h}\,\bar{F}_0}\right)^2 + \left(\frac{\bar{h}}{\bar{\mu}}\frac{\partial\bar{p}}{\partial\beta}\left(\bar{z} - \frac{\bar{F}_1}{\bar{F}_0}\right)\right)^2\right]^{1/2} \quad (6)$$

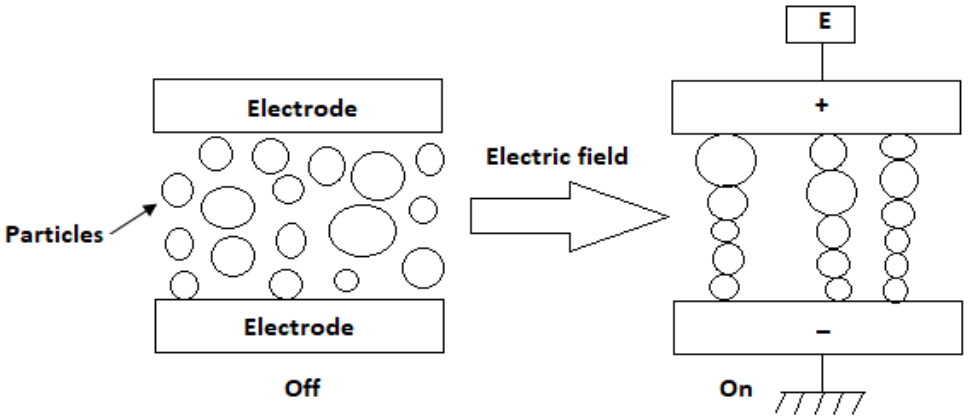

Figure 1: ERF behavior.

Table 1: Bearing parameters and lubricant properties.

Bearing Geometric Parameters		**References**
Journal Radius (mm)	50	
Radial Clearance (mm)	0.05	(Sharma et al., 1993)
Bearing Length (mm)	100	
ERF Characteristics		
Viscosity at 40°C (Pas)	0.11	(Kollias and Dimarogonas 1994)
ERF parameters:		(Nikolakopoulos and
A – fluid parameter Pa(m/V)^B	6.619x10^{-13}	Papadopoulos, 1996)
B – fluid constant	2.185	(Zhun and Ke-Qin, 2002)
Voltage (V)	0 V – 1200 V	
Operating Parameters		
Journal Speed (rpm)	2000	(Sharma et al., 1990)
Radial Load (kN)	22.4	
Supply Pressure (Pa)	8.96x10^6	

Using the bearing parameters and lubricant properties in equations (1-3), the dimensional relationship between lubricant viscosity and shear rate has been established. Equations (4-6) gives the response in non-dimensional form. The non-dimensional viscosity variation with shear rate for ERF given by Bingham model is shown in Figure 2. The apparent viscosity ($\bar{\mu}_a$) of ERF depends upon electric field strength. The applied voltage range is 400 V to 1200 V. The electric field strength is directly proportional to voltage. More the voltage, more will be the apparent

viscosity. For lower value of shear rate, viscosity variation is more and for high shear rate, the variation is less. The shear thinning behavior of lubricant viscosity has been observed for all values of voltage in the prescribed range. ERF parameter A = 6.619x10-13 Pa(m/V)^B is considered for analysis where B is constant and its value is taken as 2.185.

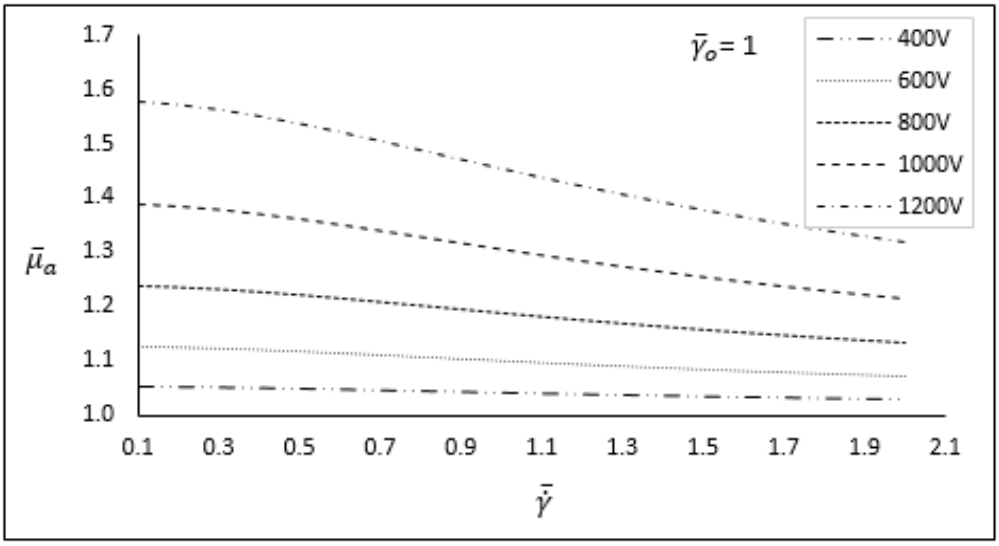

Figure 2: Viscosity variation with shear rate.

3.0 FEM FORMULATION

The non-recessed circular journal bearing system has been considered for analysis and shown in Figure 3. Non-dimensional generalized Reynold's equation governing laminar flow of incompressible lubricant considering variable viscosity can be written as eq. 7 (Fowles, 1970; Kucinschi et al., 2000):

$$\frac{\partial}{\partial\alpha}\left(\bar{h}^3\bar{F}_2\frac{\partial\bar{p}}{\partial\alpha}\right)+\frac{\partial}{\partial\beta}\left(\bar{h}^3\bar{F}_2\frac{\partial\bar{p}}{\partial\beta}\right)=\Omega\left[\frac{\partial}{\partial\alpha}\left\{\left(1-\frac{\overline{F_1}}{\overline{F_0}}\right)\bar{h}\right\}\right]+\frac{\partial\bar{h}}{\partial\bar{t}} \quad (7)$$

The dimensionless governing equation will be employed for the calculation of pressure distribution in lubricating film. In order to get the pressure field, boundary conditions for pressure will be considered.

The boundary conditions for the flow field are listed as;

(a) There is an ambient pressure at bearing edge.
(b) At internal nodes, flow is observed to be zero.
(c) Flow is non-zero on holes and external boundaries.
(d) Restrictor flow and bearing input flow are identical.

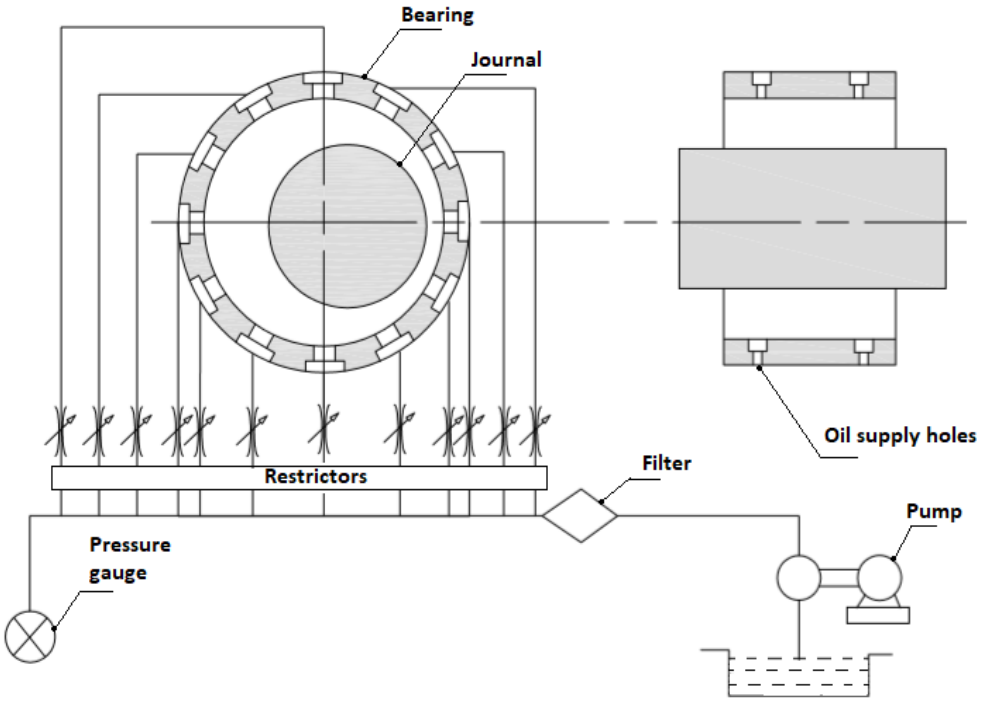

Figure 3: Non-recessed circular journal bearing system.

In present FEM analysis, the flow field is discretized for symmetric configuration as shown in Figure 4. Number of nodes are taken as 48 and number of 4-noded elements are 36. Number of holes are considered as 24 (12 in each row).

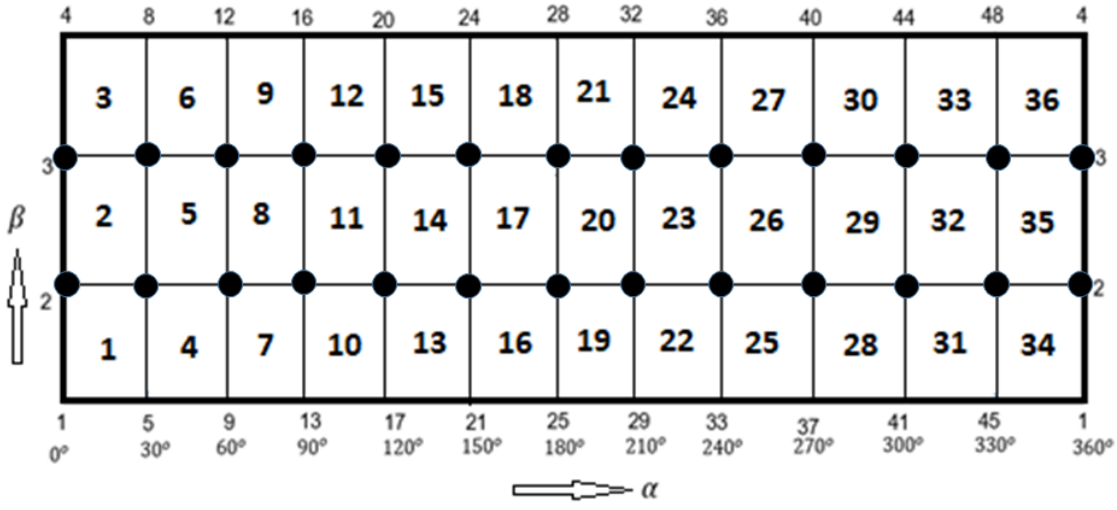

Figure 4: Flow field discretization.

The solution of Reynolds equation is obtained by Galerkin's approach of FEM and given as eq. 8.

$$[\bar{F}]\{\bar{P}\} = \{\bar{Q}\} + \Omega\{\bar{R}_H\} + \dot{\bar{X}}_J\{\bar{R}_x\} + \dot{\bar{Z}}_J\{\bar{R}_z\} \quad (8)$$

where,
$[\bar{F}]$ = assembled Fluidity Matrix,
$\{\bar{P}\}$ = nodal pressure Vector,
$\{\bar{Q}\}$ = nodal Flow Vector,
$\{\bar{R}_H\}$ = column Vectors due to hydrodynamic terms and
$\{\bar{R}_x\}$, $\{\bar{R}_z\}$ = global right hand side vector due to journal center velocities.
For eth element these are given by eq. 9 (a-e).

$$\bar{F}_{ij}{}^{e} = \int_{\Omega_e} \bar{h}^3 \left[\bar{F}_2 \frac{\partial N_i}{\partial \alpha}\frac{\partial N_j}{\partial \alpha} + \bar{F}_2 \frac{\partial N_i}{\partial \beta}\frac{\partial N_j}{\partial \beta}\right] d\Omega_e \quad (9a)$$

$$\bar{Q}_i{}^{e} = \int_{\Gamma^e} \left\{\left(\bar{h}^3 \bar{F}_2 \frac{\partial \bar{p}}{\partial \alpha} - \Omega\left(1 - \frac{\bar{F}_1}{\bar{F}_0}\right)\bar{h}\right) l_1 + \left(\bar{h}^3 \bar{F}_2 \frac{\partial \bar{p}}{\partial \beta}\right) l_2\right\} N_i d\bar{\Gamma}^e \quad (9b)$$

$$\bar{R}_{Hi}{}^{e} = \int_{\Omega_e} \left(1 - \frac{\bar{F}_1}{\bar{F}_0}\right)\bar{h}\ \frac{\partial N_i}{\partial \alpha} d\Omega_e \quad (9c)$$

$$\bar{R}_{xi}{}^{e} = \int_{\Omega_e} N_i \cos\alpha\, d\Omega_e \quad (9d)$$

$$\bar{R}_{zi}{}^{e} = \int_{\Omega_e} N_i \sin\alpha\, d\Omega_e \quad (9e)$$

Orifice restrictor is considered as a flow control device in present study. It creates the pressure difference between lubricant supply line and at the entry of bearing hole. For each hole, separate restrictor is provided. The flow through orifice restrictor can be obtained from eq. 10.

$$\bar{Q}_R = \bar{C}_{s2}(1 - \bar{p}_c)^{1/2} \quad (10)$$

where $\bar{p}_c$ is the pressure at bearing hole.

The fluid film pressure, fluid film thickness, load carrying capacity etc. fall in this category.

Fluid Film Pressure

The pressure values are obtained by eq. 11;

$$\bar{p} = \sum_{j=1}^{n_l^e} \bar{p}_j N_j \quad (11)$$

Fluid Film Thickness

Fluid film thickness can be obtained by the expression given in eq. 12;

$$\bar{h} = 1 - \overline{X_J}\cos\alpha - \overline{Z_J}\ \sin\alpha \quad (12)$$

where $\overline{X_J}$ and $\overline{Z_J}$ are the journal center coordinates.

Load carrying capacity

The resulting fluid film reaction is expressed as eq. 13.

$$F = [\bar{F}_x^2 - \bar{F}_z^2]^{1/2} \quad (13)$$

Eccentricity Ratio

Eccentricity ratio is given as eq. 14.

$$\varepsilon = \sqrt{\left|\overline{X_J}\right|^2 + \left|\overline{Z_J}\right|^2} \tag{14}$$

4.0 FEM SOLUTION

The journal bearing solution procedure using FEM is shown as a flow chart in Figure 5. The input data such as journal speed, applied load, viscosity of fluid, number of elements, number of nodes etc. is computed to achieve fluid film thickness for initial journal center coordinate position. Fluidity matrix is generated and solved for the ERF. Lubricant film pressure has been obtained using boundary conditions for lubricant flow field. Iterative procedure is done to achieve journal equilibrium for applied radial load ($\overline{W}$). Increments in journal centre coordinates are computed to achieve the convergence criteria i.e., PERR<0.001. Finally, the performance characteristics has been obtained for the hybrid journal bearing system operated with ERF.

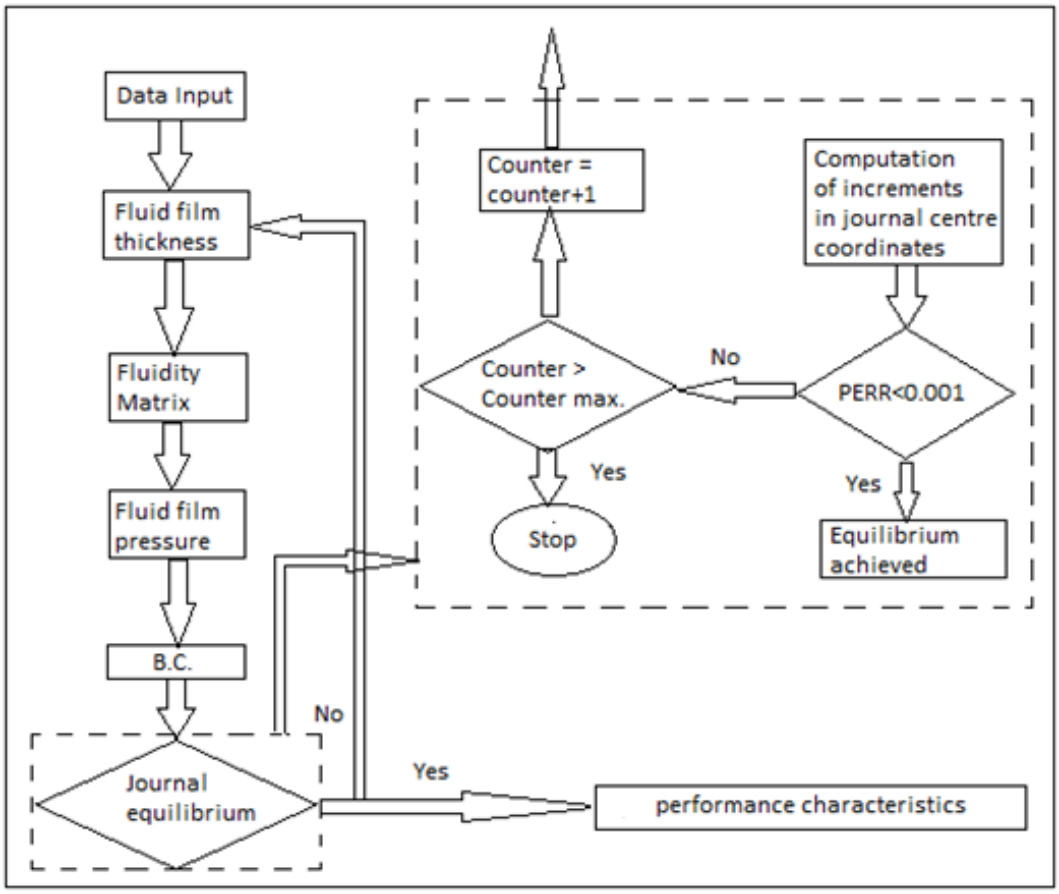

Figure 5: Journal bearing solution procedure using FEM.

The present mathematical model for hole entry hybrid journal bearing system is validated with published literature before using it to analyze the performance characteristics. Values of minimum fluid film thickness ($\bar{h}_{min}$) with respect to restrictor design parameter ($\bar{C}_{s2}$) are solved

using finite element method (FEM) and then compared with literature data (Sharma et al., 2003) as shown in Figure 6. This graph shows the decrease in $\bar{h}_{min}$ with the increase in $\bar{C}_{s2}$. The current results for $\bar{h}_{min}$ are very close to literature for the values for $\bar{C}_{s2}$ as 0.08-0.13. Slight variations in $\bar{h}_{min}$ values have been observed. Also $\bar{h}_{min}$ values decrease with increase in $\bar{W}$ (Kumar et al., 2020c).

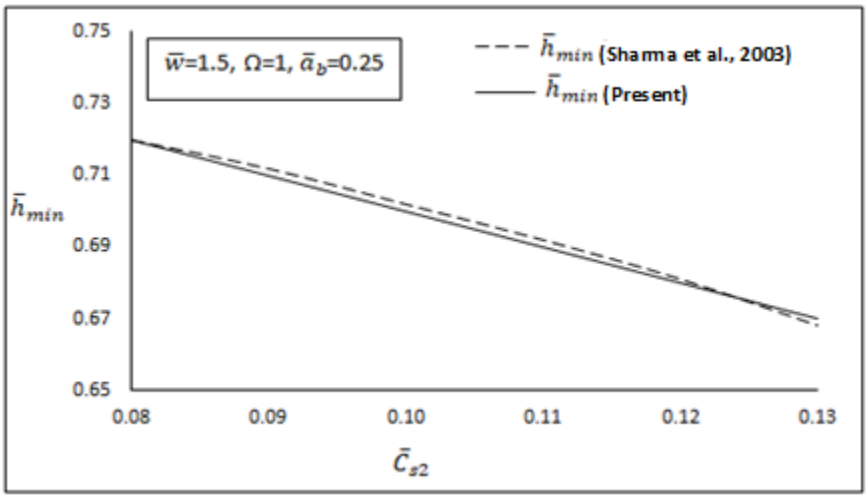

Figure 6: Variation of $\bar{h}_{min}$ with $\bar{C}_{s2}$ for FEM model validation.

5.0 RESULTS AND DISCUSSION

For symmetric hole entry configuration, performance characteristics are analyzed considering orifice restrictor as a flow control device. The variation of these performance characteristics are shown for different load ($\bar{W}$) and restrictor design parameter ($\bar{C}_{s2}$) values. Pressure distribution curves are plotted against the circumference of journal bearing. The results are compared and discussed in this section in the light of available literature. The future scope is also discussed at the end of this section.

5.1 Variations with Radial Load

The increase in $\bar{p}_{max}$ with respect to $\bar{W}$ is observed for 0 V to 1200 V as shown in Figure 7. More the electrical field strength, more will be the $\bar{p}_{max}$. For ER fluid, values of $\bar{p}_{max}$ are high as compared to Newtonian lubricant. The increase in $\bar{p}_{max}$ is 1.12% at 400 V and 10% at 1200 V compared to Newtonian lubricant for $\bar{W}$ as 1.2. The decrease in $\bar{h}_{min}$ with respect to $\bar{W}$ is shown in Figure 8. More the electrical field strength, less will be the $\bar{h}_{min}$. For ER fluid, the values of $\bar{h}_{min}$ are low as compared to Newtonian lubricant. At high $\bar{W}$, the ER effect is more for $\bar{h}_{min}$ compared to low $\bar{W}$. The increase in $\bar{Q}$ with respect to $\bar{W}$ is shown in Figure 9. More the electrical field strength, less will be the $\bar{Q}$. For ER fluid, the values of $\bar{Q}$ are low as compared to Newtonian lubricant. The decrease in $\bar{Q}$ is 3.3% at 400 V and 12.6% at 1200 V compared to Newtonian lubricant for $\bar{W}$ as 1.2. Variation of ε w.r.t. $\bar{W}$ is shown in Figure 10. It has been observed that the eccentricity ratio increases with increase in load. Values of ε are high for ER fluid at 1200 V and low for Newtonian lubricant.

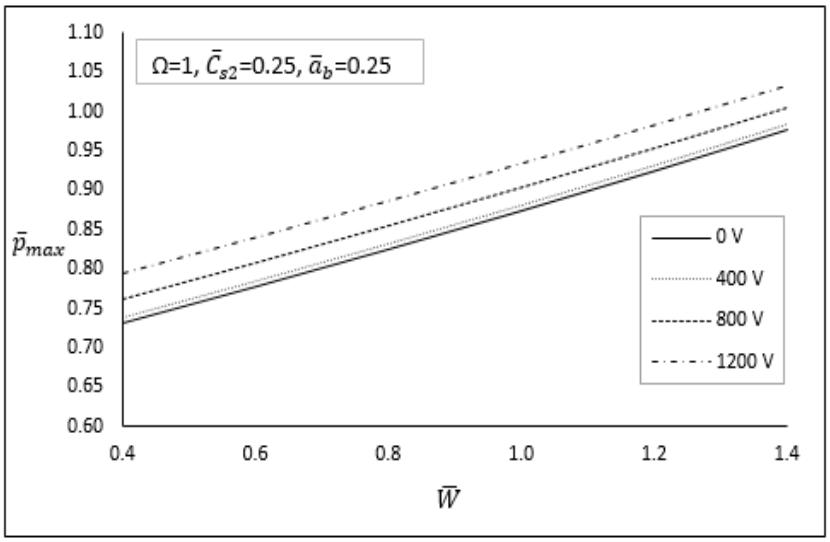

Figure 7: Variation of $\bar{p}_{max}$ w.r.t. $\bar{W}$.

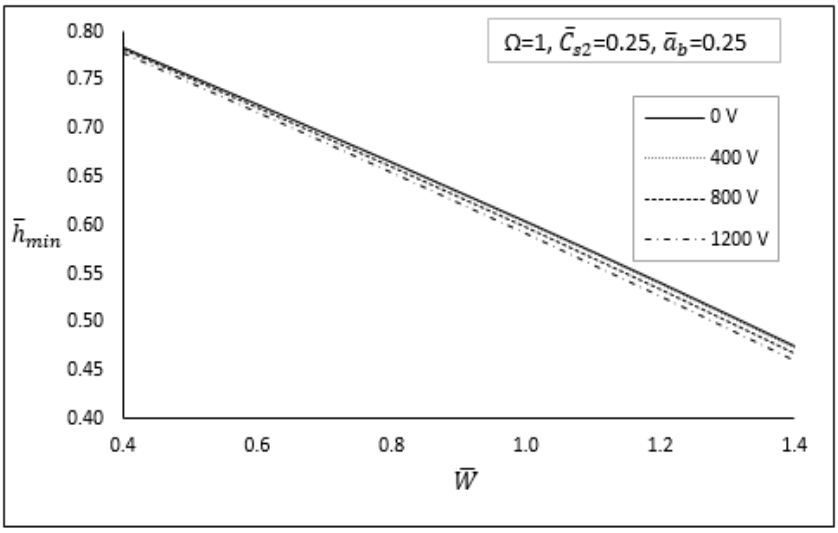

Figure 8: Variation of $\bar{h}_{min}$ w.r.t. $\bar{W}$.

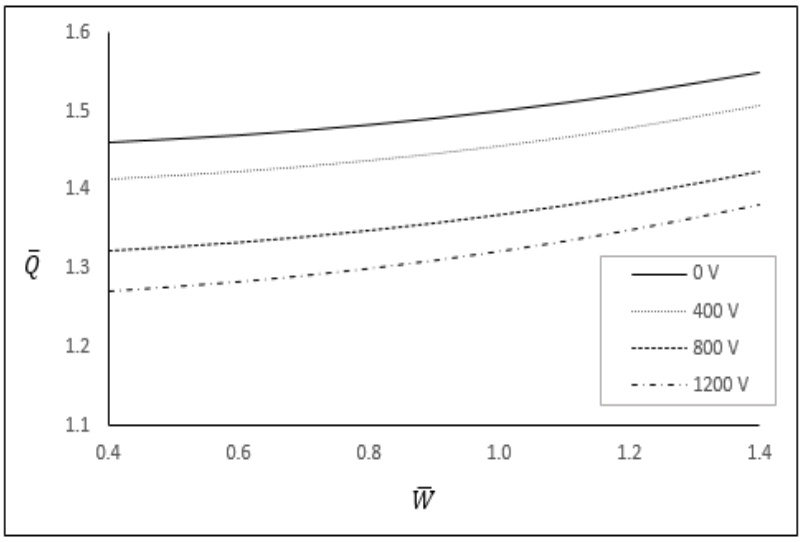

Figure 9: Variation of $\bar{Q}$ w.r.t. $\bar{W}$.

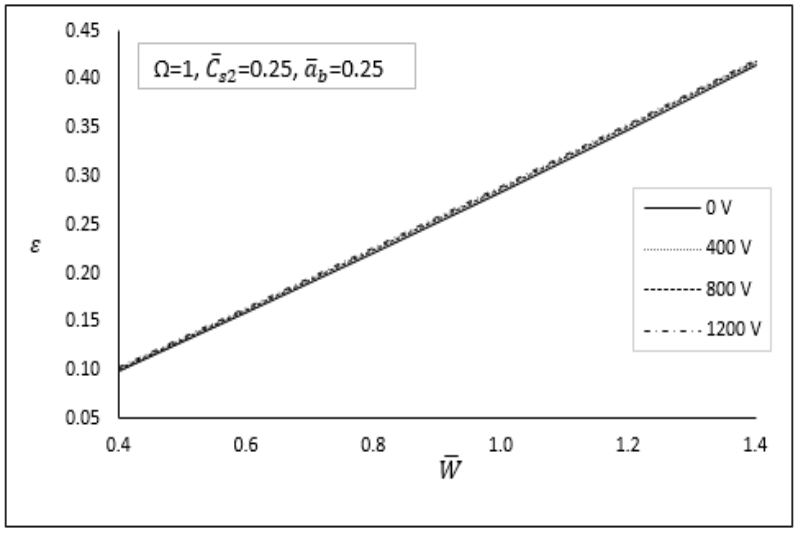

Figure 10: Variation of ε w.r.t. $\bar{W}$.

5.2 Variations with Restrictor Design Parameter

The increase in $\bar{p}_{max}$ with respect to $\bar{C}_{s2}$ is observed for 0 V to 1200 V as shown in Figure 11. More the electrical field strength, more will be the $\bar{p}_{max}$. For ER fluid, the values of $\bar{p}_{max}$ are high as compared to Newtonian lubricant. The increase in $\bar{p}_{max}$ is 1.1% at 400 V and 16% at 1200 V compared to Newtonian lubricant for $\bar{C}_{s2}$ as 0.12. The decrease in $\bar{h}_{min}$ with respect to $\bar{C}_{s2}$ is observed for 0 V to 1200 V and shown in Figure 12. More the electrical field strength, more will be $\bar{h}_{min}$. The values of $\bar{h}_{min}$ are high for ER fluid as compared to Newtonian lubricant and ER effect is predominant at low value of $\bar{C}_{s2}$.

The increase in $\bar{Q}$ with respect to $\bar{C}_{s2}$ is observed for 0 V to 1200 V as shown in Figure 13. More the electrical field strength, less will be the $\bar{Q}$. For ER fluid, the values of $\bar{Q}$ are low as compared to Newtonian lubricant. The decrease in $\bar{Q}$ is 3.5% at 400 V and 11.4% at 1200 V compared to Newtonian lubricant for $\bar{C}_{s2}$ as 0.12.

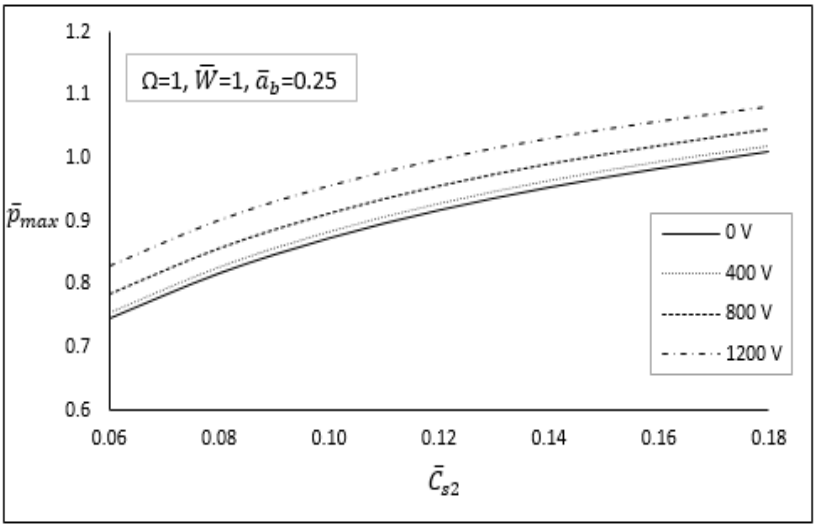

Figure 11: Variation of $\bar{p}_{max}$ w.r.t. $\bar{C}_{s2}$.

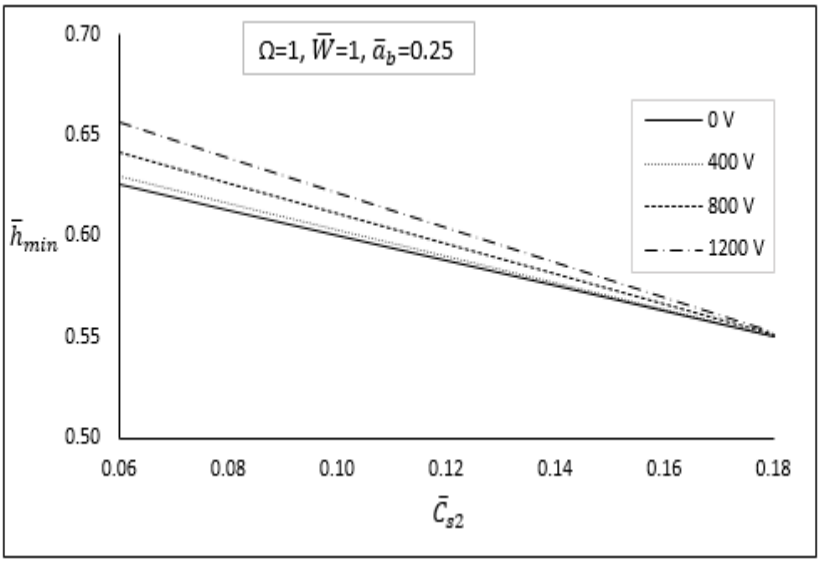

Figure 12: Variation of $\bar{h}_{min}$ w.r.t. $\bar{C}_{s2}$.

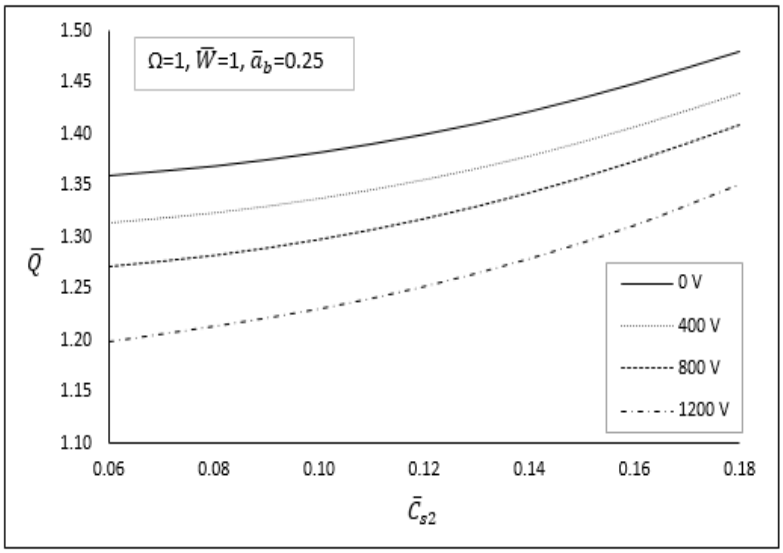

Figure 13: Variation of $\bar{Q}$ w.r.t. $\bar{C}_{s2}$.

5.3 Electrorheological Effect on Pressure Distribution

Pressure distribution curves are plotted against circumferential coordinate of ERF lubricated hole entry hybrid journal bearing and compared by varying the electric field. It has been observed that more the voltage, more will be the pressure. At 60° circumferential angle, the pressure is minimum and at 270°, the pressure is maximum for symmetric configuration. For Newtonian fluid (zero electric field), the pressure values are minimum. The pressure distribution for symmetric configuration orifice compensated non-recessed hole entry hybrid journal bearing is shown in Figure 14.

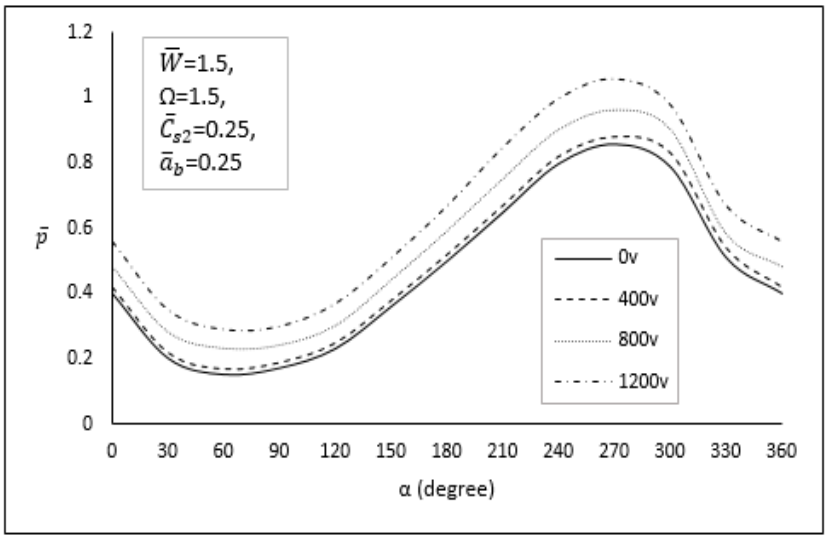

Figure 14: Pressure distribution over the bearing circumference.

The results reported in this work shows that for the suggested voltage range (0 V- 1200 V), the lubricant film pressure values at 1200 V are much higher at each point of the discretized fluid film domain for current journal bearing configuration. Hence, the bearing can support the higher load comparatively. When the fluid film pressure values of ERF lubricated bearing are compared to the Newtonian fluid lubricated bearing, at prescribed voltage range, the results are comparatively better. Considerable decrease in the values of bearing flow has been observed as a result of increasing electric field. This happens because the apparent viscosity of ERF increases with increase in electric field. Increased apparent viscosity affects the bearing flow. Reduction in minimum lubricant film thickness due to increase in electric field is highly beneficial for the bearing system to avoid metal to metal contact, even at higher applied radial load conditions.

Only limited research has been reported in the area of smart journal bearing in recent past. Hence, there is a large research scope for future. The literature (Sharma and Khatri, 2018; Sahu and Sharma, 2019; Tomar and Sharma, 2020) proved that better performance can be achieved for smart fluid operated bearings compared to Newtonian case. The present research is focused on non-recessed journal bearing. Similar analysis can be performed for recessed type journal bearing. Turbulence and thermal effects can also be considered for smart fluid operated journal bearings in the future research.

6.0 CONCLUSION

In the present study, the impact of ERF on the performance of symmetric journal bearing has been analyzed. The influence of ERF lubrication on the bearing compensated with orifice restrictor have been studied. Very precise control over the journal bearing performance characteristics has been achieved using ERF as lubricant. Apparent viscosity has been controlled by varying electric field. In case of orifice compensated hybrid journal bearing, the percentage increase in the value of maximum fluid film pressure ($\bar{p}_{max}$) and percentage decrease in the value of bearing flow ($\bar{Q}$) is observed to be 10% and 12.6% for symmetric configuration operating with ERF as lubricant at $\bar{W}$=1.2, Ω=1.0, $\bar{C}_{s2}$=0.25, $\bar{a}_b$=0.25, λ=1.0 and voltage=1200 V compared to Newtonian case. Pressure distribution curves shows that the pressure increases as the voltage increases over the entire circumference.

REFERENCES

Agrawal, N., & Sharma, S. C. (2021). Effect of the ER lubricant behaviour on the performance of spherical recessed hydrostatic thrust bearing. Tribology International, 153, 106621.

Basavaraja, J. S., Sharma, S. C., & Jain, S. C. (2010). A study of misaligned electrorheological fluid lubricated hole-entry hybrid journal bearing. Tribology International, 43(5-6), 1059-1064.

Conrad, H., & Sprecher, A. F. (1991). Characteristics and mechanisms of electrorheological fluids. Journal of statistical physics, 64(5), 1073-1091.

Dimarogonas, A. D., & Kollias, A. (1992). Electrorheological fluid-controlled “smart” journal bearings. Tribology Transactions, 35(4), 611-618.

Dorier, C., & Tichy, J. (1992). Behavior of a Bingham-like viscous fluid in lubrication flows. Journal of Non-Newtonian Fluid Mechanics, 45(3), 291-310.

Fowles, P. E. (1970). A simpler form of the general Reynolds equation. 92(4), 661-662.

Garg, H. C. (2015). Stability analysis of slot-entry hybrid journal bearings operating with non-Newtonian lubricant. Jurnal Tribologi, 6, 1-23.

Hao, T. (2001). Electrorheological fluids. Advanced Materials, 13(24), 1847-1857.
Hao, T. (2002). Electrorheological suspensions. Advances in colloid and interface science, 97(1-3), 1-35.
Jang, S., & Tichy, J. A. (1997). Internal damper characteristics of rotor system with submerged ER fluid journal bearing. International Journal of Rotating Machinery, 3(1), 61-71.
Kollias, A., & Dimarogonas, A. D. (1994). Electrorheological fluid flow in partial journal bearings. ASME-PUBLICATIONS-FED, 205, 69-81.
Kucinschi, B. R., Fillon, M., Fre^ne, J., & Pascovici, M. D. (2000). A transient thermoelastohydrodynamic study of steadily loaded plain journal bearings using finite element method analysis. J. Trib., 122(1), 219-226.
Kumar, A., & Sharma, S. C. (2019). Textured conical hybrid journal bearing with ER lubricant behavior. Tribology International, 129, 363-376.
Kumar, S., Kumar, V., & Singh, A. K. (2020). Influence of lubricants on the performance of journal bearings–a review. Tribology-Materials, Surfaces & Interfaces, 14(2), 67-78.
Kumar, S., Kumar, V., & Singh, A. K. (2020). Prediction of maximum pressure of journal bearing using ANN with multiple input parameters. Australian Journal of Mechanical Engineering, 1-10.
Kumar, S., Kumar, V., & Singh, A. K. (2020). Predictions of Minimum Fluid Film Thickness of Journal Bearing Using Feed-Forward Neural Network. In Proceedings of International Conference in Mechanical and Energy Technology (pp. 229-237). Springer, Singapore.
Muchammad, Tauviqirrahman, M., Soetopo, H. S. S., & Jamari (2021). Mechanical and thermal deformations effects on plain journal bearing with isoviscous boundary condition based on CFD and FSI methods. Jurnal Tribologi, 28, 63-81.
Nikolakopoulos, P. G., & Papadopoulos, C. A. (1996). High speed journal bearings lubricated with electro-rheological fluids: an experimental investigation. International Journal of Modern Physics B, 10(23n24), 3045-3055.
Nikolakopoulos, P. G., & Papadopoulos, C. A. (1998). Controllable high speed journal bearings, lubricated with electro-rheological fluids. An analytical and experimental approach. Tribology International, 31(5), 225-234.
Peng, J., & Zhu, K. Q. (2005). Hydrodynamic characteristics of ER journal bearings with external electric field imposed on the contractive part. Journal of intelligent material systems and structures, 16(6), 493-499.
Ram, N. (2016). Numerical analysis of capillary compensated micropolar fluid lubricated hole-entry journal bearings. Jurnal Tribologi, 9, 18-44.
Ram, N. (2017). Influence of couple stress lubricants on hole-entry hybrid journal bearings. Jurnal Tribologi, 14, 32-49.
Rasep, Z., Yazid, M. N. A. W. M., & Samion, S. (2021). A study of cavitation effect in a journal bearing using CFD: A case study of engine oil, palm oil and water. Jurnal Tribologi, 28, 48-62.
Sahu, K., & Sharma, S. C. (2019). Magneto-rheological fluid slot-entry journal bearing considering thermal effects. Journal of Intelligent Material Systems and Structures, 30(18-19), 2831-2852.
Sharma, S. C., & Khatri, C. B. (2018). Electro-rheological fluid lubricated textured multi-lobe hole-entry hybrid journal bearing system. Journal of Intelligent Material Systems and Structures, 29(8), 1600-1619.
Sharma, S. C., Kumar, V., Jain, S. C., & Nagaraju, T. (2003). Study of hole-entry hybrid journal bearing system considering combined influence of thermal and elastic effects. Tribology International, 36(12), 903-920.

Sharma, S. C., Sinhasan, R., & Jain, S. C. (1990). Elastohydrostatic analysis of orifice compensated multiple hole-entry hybrid journal bearings. International Journal of Machine Tools and Manufacture, 30(1), 111-129.

Sharma, S. C., Sinhasan, R., & Jain, S. C. (1993). An elastohydrostatic study of hole-entry hybrid flexible journal bearings with capillary restrictors. Tribology International, 26(2), 93-107.

Tomar, A. K., & Sharma, S. C. (2020). A Study of Hole-Entry Grooved Surface Hybrid Spherical Journal Bearing Operating with Electrorheological Lubricant. Journal of Tribology, 142(11).

Yadav, S. K., & Ram, N. (2018). Transient response of two lobe aerodynamic journal bearing. Jurnal Tribologi, 16, 1-14.

Zhun, Z., & Ke-Qin, Z. (2002). Characteristics of electrorheological fluid flow in journal bearings. Chinese physics letters, 19(2), 273.